PERFORMANCE OF THREE *QRS* DETECTION ALGORITHMS DURING SLEEP: A COMPARATIVE STUDY

Leontios J. Hadjileontiadis[1], Kostas I. Panoulas[1], Thomas Penzel[2], and Stavros M. Panas[1]
[1]Department of Electrical and Computer Engineering, Aristotle University of Thessaloniki,
GR 54006 Thessaloniki, GREECE {leontios@auth.gr}
[2]Department for Internal Medicine and Pneumology, Philipps University, D-35033 Marburg, GERMANY

***Abstract* – A comparison of the performance of three *QRS* detectors used in the analysis of electrocardiogram (ECG) during sleep is presented in this paper. Two widely used *QRS* detection algorithms based on digital filtering (DF) are compared with a newly introduced one, based on Higher-Order Statistics (HOS). The percentage of *QRS* complexes failed detection along with the number of false positives and false negatives are measured for quantitative performance evaluation. Experimental results, when applying the proposed methods to nocturnal ECG recordings from the Sleep Laboratory of the Philipps University of Marburg, Germany, prove that the HOS-based *QRS* detector exhibits higher overall *QRS* detection accuracy (99.95%) than the two DF-based ones (99.75% and 99.59%, respectively). Moreover, it has lower noise susceptibility despite the presence of different noise types, such as smooth or abrupt baseline drift, 50Hz powerline interference, electromyographic intervention or any arrhythmia effect due to sleep apnea.**

***Keywords* – ECG, *QRS* complex, digital filtering, higher-order statistics, sleep apnea, adaptive robust detector, comparative study.**

I. INTRODUCTION

AUTOMATED analysis of electrocardiogram (ECG) requires the accurate detection of *QRS* complexes despite any noise presence. Most of the existing ECG analysis algorithms are focused on the identification of the *R*-wave in the *QRS* complex, once it is accurately identified, it provides a reliable basis for the identification of the whole *QRS* complex. Physiological variability of *QRS* complexes, time-varying morphology of ECG, along with noise contamination from various noise sources increase the difficulty of the *QRS* complex identification task. Noise sources include power-line interface, muscle contraction noise, poor electrode contact, patient movement, baseline wandering due to respiration, and *T* waves with high-frequency characteristics similar to *QRS* complexes [1].

Typical approaches for most *QRS* detectors implement one or more of three different types of processing steps, i.e., linear digital filtering, nonlinear transformation, and decision rule algorithms [2]. Linear processes include a bandpass filter, a derivative, and a moving window integrator, while amplitude squaring and adaptive thresholds usually account for the nonlinear transformation and the decision rule algorithm, respectively.

The adaptation flexibility of the *QRS* detectors to accurately account for the inherent time-varying morphology of the *QRS* complex is of great importance. In the present study, the performance of three *QRS* detection schemes is quantified and compared on the basis of their adaptation ability. The two of them are structured on a digital filtering (DF) origin, namely DF1 [3], [1], and DF2 [4], and are widely used in the clinical practice. The third one, newly introduced, is based on higher-order statistics (HOS), namely HOS *R*-wave detector (HOS-RWD) [5]. The property of HOS to be zero for Gaussian signals and exhibit high values for transient non-Gaussian ones provides adaptive thresholds structured on the variation of skewness and kurtosis parameters when the *QRS* complex is present. Thus, the necessary information regarding the location of *R*-wave is extracted resulting in accurate estimates of the *QRS* complex.

Tests of the three algorithms on nocturnal ECG recordings from the Sleep Laboratory of the Philipps University of Marburg, Germany, provide a means of comparing the performance of one algorithm to another and evaluating their utility in a clinical environment.

II. OVERVIEW OF THE THREE ALGORITHMS

A. Digital Filtering-based Algorithm #1 (DF1)

This algorithm was initially introduced by Engelese and Zeelenberg [3] and later adapted by Friesen *et al.* [1]. The version used in the present study is the second one but slightly modified for eliminating high frequencies, the 50 Hz instead of the 62.5 Hz power-line interference, and further becoming independent from the choice of the sampling frequency of the ECG data.

The ECG signal $X(k), k = 1, \ldots, N$, where N is the length of each processed ECG record, is passed through a differentiator with a 50 Hz notch filter,

$$Y0(k) = X(k) - X(k - \text{int}(\frac{f_s}{50})), \text{int}(\frac{f_s}{50}) < k \le N, \quad (1)$$

where, int(·) denotes the integer part of a ratio and f_s the sampling frequency.

The differentiated, filtered data is then passed through a digital band-pass filter (FIR, 0-1 Hz stopband, 6-25 Hz passband, 35-100 Hz stopband),

$$Y1(k) = \sum_{i=0}^{p} w_i Y0(k-i), \quad (2)$$

where, *p-1* is the order of the filter and w_i is the coefficient. Two equal in magnitude but opposite in polarity thresholds are applied in the output of the bandpass filter [1]. The latter is scanned until a point with amplitude greater than the positive threshold is reached, indicating the onset of a 160 ms search region.

The number of alternate threshold crossing is used to classify the initial crossing as either a base-line shift, a *QRS* candidate, or as noise. If no other threshold crossing occurs within that search region, the occurrence is classified as a baseline shift. Otherwise, three-decision conditions are tested [1], and if anyone of them applies, the occurrence is classified

This work was partially supported by the Institution of State Scholarships of Greece (I.K.Y.) and the German Academic Exchange Program (DAAD), under the Greek-German Scientific Collaboration Programme 'IKYDA 2000 2001'.

Report Documentation Page

Report Date	Report Type	Dates Covered (from... to)
25 Oct 2001	N/A	-

Title and Subtitle Performance of Three QRS Detection Algorithms During Sleep: A Comparative Study	**Contract Number**
	Grant Number
	Program Element Number
Author(s)	**Project Number**
	Task Number
	Work Unit Number
Performing Organization Name(s) and Address(es) Department of Electrical and Computer Enginering Aristotle University of Thessaloniki GR 54006 Thessaloniki Greece	**Performing Organization Report Number**
Sponsoring/Monitoring Agency Name(s) and Address(es) US Army Research, Development & Standardization Group (UK) PSC 802 Box 15 FPO AE 09499-1500	**Sponsor/Monitor's Acronym(s)**
	Sponsor/Monitor's Report Number(s)

Distribution/Availability Statement
Approved for public release, distribution unlimited

Supplementary Notes
Papers from 23rd Annual International Conference of the IEEE Engineering in Medicine and Biology Society, October 25-28, 2001, held in Istanbul, Turkey. See also ADM001351 for entire conference on cd-rom., The original document contains color images.

Abstract

Subject Terms

Report Classification unclassified	**Classification of this page** unclassified
Classification of Abstract unclassified	**Limitation of Abstract** UU

Number of Pages
4

as a *QRS* candidate. If additional threshold crossings occur, the occurrence is classified as noise.

B. Digital Filtering-based Algorithm #2 (DF2)

This algorithm was introduced by Pan and Tompkins [4] and it is realized through a sequence of processing steps that include two digital filters, amplitude squaring, moving-window integrator, and thresholds adaptation. The algorithm had been modified for the initial steps.

At first a bandpass is used, as described by (2). Then a five-point derivative was used,

$$Y0(k) = \frac{1}{10}(2X(k-4) + X(k-3) - X(k-1) - 2X(k)). \quad (3)$$

After differentiation, the resulted signal $Y(k)$ is squared point by point

$$Y1(k) = [Y(k)]^2, \quad (4)$$

creating a nonlinear amplification of the output of the derivative emphasizing the higher frequencies. Then a moving-window integration is calculated over 150 msec.

$$Y2(k) = (1/M)[Y1(k-(M-1)) + Y1(k-(M-2)) + \\ + \cdots + Y1(k)], \quad (5)$$

where, M is the width of the moving window (M=30 samples [4] for 200 Hz sampling rate).

Finally, an adjusting procedure that automatically sets thresholds to float over the noise and successfully discriminates *QRS* complexes from noise or T-waves takes place [4].

C. HOS-based Algorithm (HOS-RWD)

Panoulas, Hadjileontiadis and Panas [5] introduced this algorithm, which is based on the advantageous properties of HOS over Gaussian noise. When the $X(k)$ signal includes transients with high amplitude its distribution shifts to a non-Gaussian one. Consequently, the two HOS parameters, i.e., skewness, γ_3^x, and kurtosis, γ_4^x, given by

$$\gamma_3^x = E\{X^3(k)\}, \quad (6)$$

$$\gamma_4^x = E\{X^4(k)\} - 3[E\{X^2(k)]^2, \quad (7)$$

exhibit high values, since they express the symmetry and the heaviness of the tail of the distribution, respectively [6]. In this way, skewness and kurtosis could be used as indices of the presence or not of a transient in the $X(k)$ signal.

Initially, a signal conditioning process takes place where amplitude normalization and DC extraction, using a high pass filter (5^{th}-order Butterworth, cut-off frequency=3Hz) of the N-sampled ECG signal $X(k)$ are performed. Then, the length L ($<<N$) of a sliding window along with the R-wave length, D, are set in accordance to the sampling frequency, f_s, as the integer part of $L=f_s/3$ and $D=0.02\cdot f_s$, respectively. In addition, initial values of the thresholds used for the HOS parameters are also selected. Next, $X(k)$ is windowed with a 99% overlap-sliding window of L samples. At each window, $\hat{\gamma}_3$ and $\hat{\gamma}_4$ are estimated using normalized versions of (6) and (7), respectively, and their values are located at the end of the window. Then, the local maxima of the first derivative of $\hat{\gamma}_3$ and $\hat{\gamma}_4$ are calculated indicating the locations of possible R-wave. Subsequently, the values of $\hat{\gamma}_3$ and $\hat{\gamma}_4$ at the possible locations are compared with two thresholds; in case they are smaller the window is shifted by one sample. If their values exceed the thresholds, the two locations are compared to each other and in case they differ the location pointed out by kurtosis is preferred [5]. Then, the thresholds are updated using the mean value of the last five maximum values of $\hat{\gamma}_3$ and $\hat{\gamma}_4$, respectively. After the estimation of the first R-wave, the window skips D samples to the right and proceeds with the next one until the end of the input data is reached.

IV. Implementation

The whole analysis was implemented on an IBM-PC (Pentium III/800 MHz) using the programming language Matlab 6.0 (The Mathworks, Inc., Natick, MA). The DF1, DF2 and HOS-RWD were applied on nocturnal ECG recordings from 4 subjects (3 normal and 1 with severe sleep apnea and cyclical variation of heart rate). The recordings took place at the Sleep Laboratory of the Philipps University of Marburg, Germany with a mean duration of 8 hrs and 35 mins (Table I). All analyzed files were sampled with a sampling frequency of f_s=200 Hz at a 16-bit digitization resolution. The values for the sliding window length and the R-wave duration of the HOS-RWD were selected as L=67 and D=4 samples, respectively. The order p-1 of the FIR filter described in (2) was equal to 15. The time offset for DF1 and DF2 was 11 and 24 samples, respectively.

V. Results and Discussion

Several examples of analysis results are shown in Figs. 1-4. In all these figures the 'O'-dashed, '*'-dashed-dotted and '◊'-dotted vertical lines, called hereafter *loc*-lines, mark the locations of R-waves when identified by the DF1, DF2 and HOS-RWD algorithms, respectively.

Fig. 1 depicts a 2048-sample section from file '1(N)' (Table I), which clearly notates a baseline wandering in ECG recordings. From the comparison of the *loc*-lines it is clear that DF1and HOS-RWD overcomes the effect of the baseline wandering and accurately find the true locations of all 9 R-waves included in that section. On the other hand, DF2 is quite affected by the baseline drift and misidentifies 2 from the 9 R-waves.

Fig. 2 shows a 2048-sample section from file '2(N)' (Table I) and illustrates a case of ECG with a deep S-wave in the *QRS* complex. In this case there is always the risk of misidentification of the true location of the R-wave due to the sharp S-wave peak. By careful examination of the *loc*-lines in Fig. 2 it is clear that, for all 11 *QRS* complexes included in

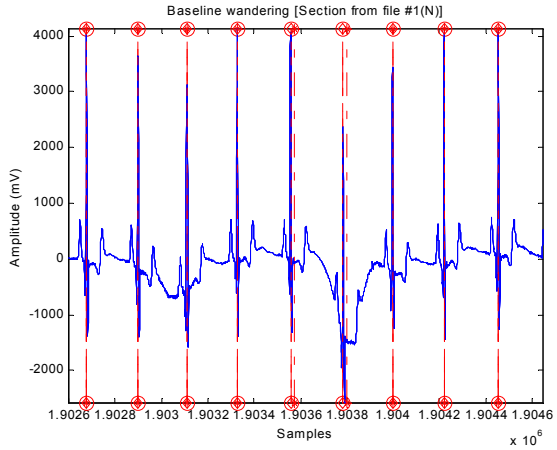

Fig. 1. A 2048-sample ECG section from file '1(N)' with baseline wandering. The *loc*-lines indicate the estimates of *R*-wave locations from DF1 ('O'--), DF2 ('*'-.), and HOS-RWD ('◊'--) algorithms, respectively.

that section the *R*-wave locations identified by DF1 are shifted to the right of the true *R*-wave peaks, coinciding with the *S*-wave locations. This indicates a severe influence of the presence of deep *S*-waves to the performance of DF1. The performance of DF2 was less affected by the presence of deep *S*-waves since 2 from 11 *R*-wave locations were not correctly found. Regarding the HOS-RWD algorithm, despite the presence of deep *S*-waves it correctly identified all 11 *R*-wave locations.

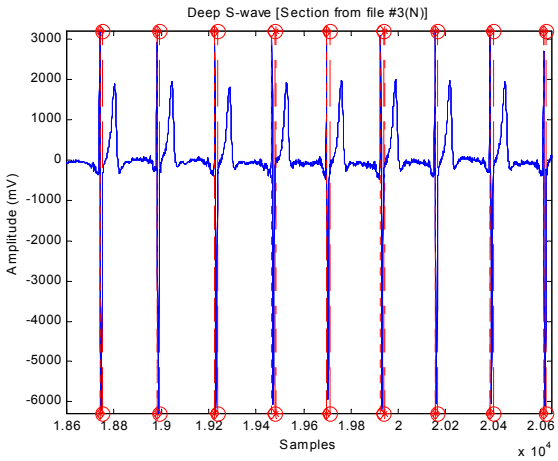

Fig. 2. A 2048-sample ECG section from file '3(N)' with deep *S*-wave. The *loc*-lines indicate the estimates of *R*-wave locations from DF1 ('O'--), DF2 ('*'-.), and HOS-RWD ('◊'--) algorithms, respectively.

Fig. 3 shows a 2048-sample section from file '4(A)' (Table I), where an arrhythmia episode is present (after the 3rd *QRS* complex). When comparing the location of the *loc*-lines it is clear that the DF1 and HOS-RWD overcome the arrhythmia effect and accurately identify the true locations of all 10 *R*-waves included in that section. On the other hand, the performance of the DF2 algorithm is affected by the presence of arrhythmia, since it starts misallocating the true locations of *R*-waves when the *R*-*R* time interval varies due to arrhythmia (especially after the 5th *QRS* complex). Furthermore, this figure also shows an *R*-wave that unlike

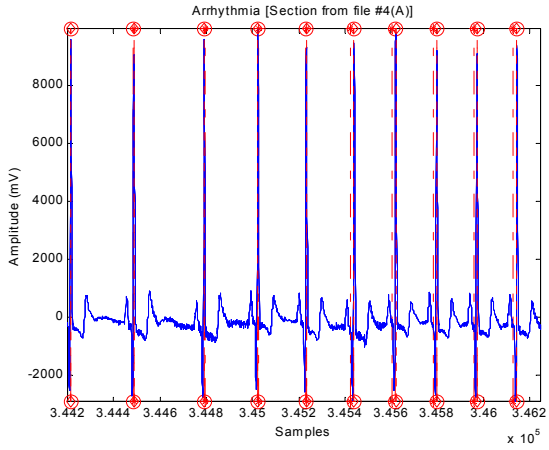

Fig. 3. A 2048-sample ECG section from file '4(A)' with an arrhythmia effect. The *loc*-lines indicate the estimates of *R*-wave locations from DF1 ('O'--), DF2 ('*'-.), and HOS-RWD ('◊'--) algorithms, respectively.

DF1 and HOS-RWD failed detection by the DF2 algorithm (1st *QRS* complex).

Fig. 4 illustrates a noisy 2048-sample ECG recording, taken from another part of file '4(A)', where apart from the existence of arrhythmia there is a high-frequency noise contamination. The simultaneous presence of the aforementioned factors deteriorates the performance of the DF2 algorithm resulting in overestimation of the true number of *R*-waves, producing false negative ones. Noise affects less the performance of DF1 and leaves unaffected the one of HOS RWD. The latter is due to the property of skewness and kurtosis to become equal to zero for Gaussian distributed

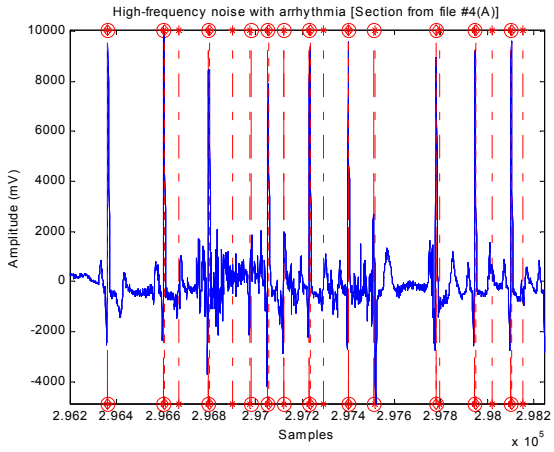

Fig. 4. A 2048-sample ECG section from file '4(A)' corrupted by high-frequency noise and also including arrhythmia effects. The *loc*-lines indicate the estimates of *R*-wave locations from DF1 ('O'--), DF2 ('*'-.), and HOS-RWD ('◊'--) algorithms, respectively.

random processes, such as additive Gaussian noise [5].

Apart from the qualitative evaluation of the results by visual examination of Figs. 1-4, a quantitative analysis was also performed. For the quantitative evaluation of the efficiency of DF1, DF2 and HOS-RWD, the numbers of false positive *R*-waves (FP), false negative (FN) and the number of *R*-waves that failed detection (FD) were calculated separately and overall for all analyzed ECG records. These evaluators describe the ability of these three algorithms to find the

TABLE I
PERFORMANCE OF THE DF1, DF2 AND HOS RWD ALGORITHMS WHEN APPLIED ON ECGS RECORDED FROM FOUR SLEEPING SUBJECTS

ECG Records	Record Duration (hrs:min)	Total (No. of [a]B)	[a]FP (B)	[a]FN (B)	[a]FD (B)	FD (%)	FP (B)	FN (B)	FD (B)	FD (%)	FP (B)	FN (B)	FD (B)	FD (%)
			DF1				DF2				HOS-RWD			
1 ([a]N)	7:39	24800	10	42	7	0.02	520	220	69	0.27	2	0	14	0.05
2 (N)	9:04	30905	27	488	251	0.81	319	510	51	0.16	21	582	17	0.05
3 (N)	7:37	21652	1292	23	4	0.01	888	224	20	0.09	0	0	4	0.01
4 ([a]A)	8:19	31078	53	672	11	0.03	831	300	310	0.99	0	1	26	0.08
Totals	33:16	108435	1382	1225	273	0.25	2558	1254	450	0.41	23	583	61	0.05

[a]N: Normal, A: Apneic; B: Beats; FP: False Positive, FN: False Negative, FD: Failed Detection.

correct number of *R*-waves without producing any overestimation (FN) or underestimation (FD) of their number, at the correct position in the raw data without misallocating them (FP).

Analytical results for the quantitative evaluators for each case and overall are shown in Table I. These results indicate that the HOS-RWD is the most efficient among the three examined algorithms in accurately detecting the *QRS* complexes, since it exhibits the lowest errors. In particular, HOS RWD has the lowest overall FP (0.021%), FN (0.53%) and FD (0.05%) values from the other two algorithms. The DF1 algorithm is ranked second, since it exhibits less errors than the DF2 algorithm overall, FP (1.27%), FN (1.13%), FD (0.25%), and FP (2.36%), FN (1.15%), FD (0.41%), respectively. Comparing the individual performances of the three algorithms for each ECG record of Table I it can be noticed that the DF1 algorithm has smaller FD values than the ones of HOS-RWD in two cases [files '1(N) and '4(A)'], but significantly higher FP and FN values. This indicates that although DF1 missed fewer *QRS* complexes than the HOS-RWD it overestimated their true number and in some cases it misallocated them. Consequently, despite some small loses in the identified *QRS* complexes, the HOS-RWD performs more accurately than the DF1 in the individual cases analyzed. The DF2 algorithm has smaller FD values than the ones of DF1 only in one case [file '2(N)'] but higher FP and FP values for the same case. Furthermore, DF2 exhibits smaller FP and FN values than the ones of DF1 only in cases '3(N)' and '4(A)', respectively, but has higher FN, FP and FD values for the same cases. Thus, DF1 performs quite better than the DF2 algorithm in the different cases examined.

From the above results, it can be seen that all three algorithms successfully identified a large percentage of the total number of *QRS* complexes, indicating that all of them could adapt to the characteristics of nocturnal ECG recordings, especially those seen in sleep apnea, such as cyclical heart rate variation. Thus, they all could be used in a clinical practice. Nevertheless, from the three algorithms examined, the HOS-RWD has the lowest overall performance errors and the lowest susceptibility either in baseline wandering and/or presence of deep *S*-waves and/or arrhythmia effect and/or additive high-frequency noise. Consequently, the HOS-RWD shows evidences of a very promising *QRS* complex detector scheme that successfully could be applied in clinical or ambulatory heart rate screening and give rise to more accurate analysis of heart rate variability.

VI. CONCLUSION

Three *QRS* detection algorithms were compared and evaluated through their performance on nocturnal ECG recordings analysis. The two of them, DF1 and DF2, widely used, are based on digital filtering, while the third one, HOS-RWD, is based on higher-order statistics and it is newly introduced. Quantitative and qualitative analysis of the results obtained from the analysis of nocturnal ECGs recorded from normal and apneic subjects show reliable and accurate performance from all three *QRS* detectors. Nevertheless, the HOS RWD performs better than the other two ones, since it exhibits the lowest performance errors. Additionally, it is not affected by noise contamination of the ECG data capturing more accurately the spectral/temporal variations in *QRS* morphology due to the properties of its employed HOS-based parameters. Finally, the HOS-RWD algorithm overcomes more efficiently than the DF1 and DF2 schemes the heart rate disorders seen in nocturnal ECG recordings, especially during apnea episodes.

REFERENCES

[1] G. M. Friesen, T. C. Jannett, M. A. Jadallah, S. L. Yates, S. R. Quint, and H. R. Nagle, "A comparison of the noise sensitivity of nine *QRS* detection algorithms," *IEEE Trans. Biomed. Eng.,* vol. 37, pp. 85-98, Jan. 1990.

[2] O. Pahlm and L. Sornmo, "Software *QRS* detection in amburatory monitoring-A review," *Med. Biol. Eng. Comput.* vol. 22, pp. 289-297, 1984.

[3] W. A. H. Englese and C. Zeelenberg, "A single scan algorithm for QRS-detection and feature extraction," *IEEE Comput. Card.*, Long Beach: IEEE Computer Society, pp. 37-42, 1979.

[4] J. Pan and W. J. Tompkins, "A real-time *QRS* detection algorithm," *IEEE Trans. Biomed. Eng.*, vol. 32, pp. 230-236, March 1985.

[5] K. I. Panoulas, L. J. Hadjileontiadis, and S. M. Panas, "Enhancement of *R*-wave detection in ECG data analysis using higher-order statistics," 23rd Annual International Conference of the IEEE EMBS, 25-28 October, Istanbul, Turkey, 2001, *submitted.*

[6] Ch. L. Nikias and A. M. Petropulu, *Higher-Order Spectra Analysis: A nonlinear signal processing framework,* New Jersey: PTR Prentice-Hall, Inc., USA, 1993, pp. 7-19.